

UDC 669.018+ 539.216.2

O. I. Kushnerov*, V. F. Bashev

Oles Honchar Dnipropetrovsk National University, Dnipropetrovsk, Ukraine

**e-mail: kushnerev@gmail.com*

STRUCTURE AND MECHANICAL PROPERTIES OF Al-Co-Cr-Fe-Mn-Ni-Si-V HIGH-ENTROPY ALLOYS IN THE AS-CAST AND SPLAT-QUENCHED STATE

The multicomponent high-entropy alloys of Al-Co-Cr-Fe-Mn-Ni-Si-V system in the as-cast and splat-quenched state were investigated. Phase formation criteria for high-entropy alloys were considered. Effect of the concentration of valence electrons in the alloy to form a solid solution structure was examined. The as-cast alloys show a multiphase BCC+B2 structure, while the splat-quenched - fully disordered BCC crystal structure only. The value of lattice parameters of the investigated alloys suggests that the solid solutions are form on the base of Cr lattice, in view of its higher melting temperature. All of the as-cast alloys display a typical cast dendritic structure with various configurations and volumes of the interdendritic space. The positive influence of microstrains level and dislocation density on the microhardness values of splat-quenched Al-Co-Cr-Fe-Mn-Ni-Si-V alloys has been established. Improved mechanical characteristics are ensured by the strong distortion of the crystal lattice due to the differences in atomic radii of the elements.

Keywords: multicomponent high-entropy alloy, structure, microhardness, splat-quenching.

Досліджено багатокомпонентні високоентропійні сплави системи Al-Co-Cr-Fe-Mn-Ni-Si-V. Розглянуто критерії, що дозволяють прогнозувати фазовий склад сплавів. Розглянуто вплив концентрації валентних електронів в сплаві на структуру твердого розчину, що утворюється в них. Встановлено, що литі сплави мають багатофазну структуру, в якій наявні тверді розчини із решіткою типу ОЦК та впорядковані тверді розчини структурного типу В2, в той час, як у рідкозагартованих сплавах, наявні лише неупорядковані тверді розчини типу ОЦК. Значення параметрів решітки вказують на те, що в якості основи для формування твердих розчинів слід розглядати решітку Cr, як елемента з найбільшою температурою плавлення. Встановлено, що досліджені сплави мають типову дендритну структуру із різними конфігураціями та об'ємами міждендритного простору. Показано, що збільшення рівня мікронапружень та густини дислокацій при гартуванні з рідкого стану сприяють підвищенню механічних характеристик досліджених сплавів. Підвищення міцності відбувається завдяки значному викривленню кристалічної решітки внаслідок відмінності атомних радіусів елементів.

Ключові слова: високоентропійний сплав, структура, мікротвердість, гартування з рідкого стану.

Исследованы многокомпонентные высокоэнтропийные сплавы системы Al-Co-Cr-Fe-Mn-Ni-Si-V в литом и жидкозакаленном состоянии. Рассмотрены критерии, позволяющие прогнозировать фазовый состав высокоэнтропийных сплавов. Рассмотрено влияние концентрации валентных электронов в сплаве на структуру образующегося твердого раствора. Установлено, что литые сплавы имеют многофазную структуру, в которой присутствуют твердые растворы с решеткой типа ОЦК и упорядоченные твердые растворы структурного типа В2, в то время, как в жидкозакаленных сплавах фиксируются только неупорядоченные твердые растворы типа ОЦК. Значения параметров кристаллической решетки указывают на то, что основой для формирования указанных твердых растворов является решетка Cr, как элемента с наибольшей температурой плавления. Установлено, что изученные сплавы имеют типичную дендритную структуру с различными конфигурациями и объемами междендритного пространства. Показано, что повышение уровня микронапряжений и плотности дислокаций при закалке из жидкого состояния способствуют повышению механических характеристик исследованных сплавов. Повышенные прочностные характеристики обусловлены сильным искажением кристаллической решетки вследствие различий в атомных радиусах элементов.

Ключевые слова: высокоэнтропийный сплав, структура, микротвердость, закалка из жидкого состояния

1. Introduction

The conventional development of new alloys is based on one or two elements as major constituents, and some other minor elements for the optimization of final properties. Recently a new class of materials known in the literature as multicomponent high-entropy alloys (HEA's) was obtained [1]. High-entropy alloys are defined as solid solution alloys that contain more than five principal elements (usually from five to thirteen) in equal or near equal atomic percents. The basic principle of HEA's is a stabilization of solution phase by the significantly higher configurational entropy of mixing ΔS_{mix} compared to conventional alloys. The configurational entropy of mixing during the formation of regular solution alloy can be determined as

$$\Delta S_{mix} = -R \sum_{i=1}^n c_i \ln c_i, \quad (1)$$

c_i is an atomic fraction of the i -th component, R is the universal gas constant. An increase of mixing entropy reduces the Gibbs free energy of the alloy and improves the stability of the solid solution. The mixing entropy reaches a maximum at equal atomic fractions of mixed components (for alloy with n components). The value of ΔS_{mix} is in the range of 12-19 J/(mol·K) usually in HEA's. Due to the high mixing entropy HEA's are solid solutions having typically simple crystal structures (FCC or BCC), but to avoid the appearance of brittle intermetallic compounds, complex microstructures and amorphous phases in the structure of alloys, some phase formation criteria are required to be completed. According to [2, 3], the Ω parameter can be used to estimate the phase composition of HEA.

$$\Omega = \frac{T_m \Delta S_{mix}}{|\Delta H_{mix}|} \quad (2)$$

where T_m is the average melting temperature of alloy and ΔH_{mix} - mixing enthalpy

$$T_m = \sum_{i=1}^n c_i (T_m)_i, \quad (3)$$

$$\Delta H_{mix} = \sum_{i=1, i \neq j}^n \Omega_{ij} c_i c_j \quad (4)$$

where the regular melt-interaction parameter between i -th and j -th elements $\Omega_{ij} = 4\Delta H_{mix}^{AB}$, and ΔH_{mix}^{AB} - mixing enthalpy of binary liquid AB alloy. Alloy components should not have large atomic-size difference, which is described by the parameter

$$\delta = 100 \sqrt{\sum_{i=1}^n c_i \left(1 - \frac{r_i}{\bar{r}}\right)^2} \quad (5)$$

where $\bar{r} = \sum_{i=1}^n c_i r_i$, r_i - the atomic radius of the i -th element.

According to [2], the HEA's for which $\Omega \geq 1.1$ and $\delta \leq 6.6$ can form the solid solutions without intermetallic compounds and amorphous phases. However, simple (not ordered) solid solutions form if $-15 \text{ kJ/mol} < \Delta H_{mix} < 5 \text{ kJ/mol}$ and $\delta \leq 4.6$.

The other useful parameter is a valence electron concentration, VEC , which has been proven useful in determining the phase stability of HEA's [4, 5]. VEC is defined as follows

$$VEC = \sum_{i=1}^n c_i (VEC)_i \quad (6)$$

where $(VEC)_i$ is a valence electron concentration (including the d -electrons) of the i -th element. As pointed in [5] at $VEC \geq 8.0$, sole FCC phase exists in alloy; at $6.87 \leq VEC < 8.0$, mixed FCC and BCC phases will co-exist and sole BCC phase exists at $VEC < 6.87$.

HEA's possess many attractive properties, such as high hardness, outstanding wear resistance, irradiation resistance, excellent high-temperature strength, good thermal stability and corrosion resistance [1, 6-9]. Improved mechanical characteristics are ensured by the strong distortion of the crystal lattice due to the differences in atomic radii of the elements.

In the work an effect of mixing entropy and composition on microhardness, phase composition and parameters of the fine structure of HEA's of Al-Co-Cr-Fe-Mn-Ni-Si-V alloy system is discussed (Mn and Si are added as minor elements in order to improve mechanical properties and corrosion resistance).

2. Experimental details

The samples of Al-Co-Cr-Fe-Mn-Ni-Si-V high-entropy alloys were taken from the as-cast (cooling rate of $\sim 10^2 \text{ K}\cdot\text{s}^{-1}$) ingots, polished and etched for examining the microstructure under an optical microscope Neophot-21 and scanning electron microscope (SEM, JSM-6490LV) with energy dispersive spectrometry (EDS). The quenching from the molten state (splat-quenching, SQ) was performed using the well-known technique of melt spinning, i.e., spreading of melt droplets on the internal surface of a rapidly rotating copper cylinder. The rate of cooling as estimated from the thickness of the obtained foils was $\sim 10^5\text{--}10^6 \text{ K/s}$. The XRD studies were carried out with the use of DRON-2.0 X-ray diffractometer in Cu $K\alpha$ monochromatized radiation. The microhardness was measured on a PMT-3 microhardness-meter at a load of 200 g.

3. Results and discussion

Using the data listed in Tab.1 and Tab. 2., the following quantities are calculated for the HEAs (as listed in Tab. 3): ΔS_{mix} , ΔH_{mix} , δ , Ω and VEC .

The phase composition of the investigated alloys, crystal lattice parameters and the fine structure parameters (coherent scattering areas and microstrains) (Tab.4) were determined from the XRD patterns (Fig.1, 2). The dislocation density (ρ) was obtained from the profile of the first diffraction peak (Tab.4).

Table 1

Atomic radii of elements and valence electron concentrations [4,10] of HEAs of Al-Co-Cr-Fe-Mn-Ni-Si-V alloy system

| | Al | Co | Cr | Fe | Ni | V | Si | Mn |
|-------------------|-------|-------|-------|-------|-------|-------|-------|-------|
| Atomic radii, nm. | 0.143 | 0.125 | 0.129 | 0.126 | 0.125 | 0.135 | 0.118 | 0.137 |
| VEC | 3 | 9 | 6 | 8 | 10 | 5 | 4 | 7 |

The analysis of the XRD patterns allowed us to establish what the investigated HEAs in the as-cast state have two-phase BCC + B2 (CsCl) structure. Indeed, from the analyses of Tab. 3 it is seen that ΔH_{mix} has a large negative value favoring the formation of a compound. The low value of VEC favors the formation of a BCC phase. These factors put together leads to the formation of a mixture of BCC and B2 phases (the ordered version of BCC). Exception is the $\text{AlCoCrFe}_{1.87}\text{Mn}_{0.03}\text{NiSi}_{0.1}\text{V}$ alloy, for which the value of VEC lies in the range where a FCC + BCC mixture is favored. But, as pointed in [11], if the value of VEC is close to the boundary values, predictions of the phase compositions sometimes does not work.

Meanwhile the XRD patterns of SQ alloys do not have a (100) B2 superlattice reflection and, consequently, SQ HEA's only contain a disordered BCC phase. In our opinion, the high

cooling rate during the formation of thin SQ film should prevent it from possible separation and hinder the appearance of structures and phases, typical for equilibrium as-cast states.

The values of lattice parameters of the investigated alloys suggests that the solid solutions are form on the base of Cr lattice ($a = 0.2884$ nm), in view of its higher melting temperature.

Table 2 Values of ΔH_{mix}^{AB} (kJ/mol), calculated

| by Miedema's model [10] | | | | | | | |
|-------------------------|-----|-----|-----|-----|-----|-----|-----|
| Element | Co | Cr | Fe | Ni | V | Si | Mn |
| Al | -19 | -10 | -11 | -22 | -16 | -19 | -19 |
| Co | | -4 | -1 | 0 | -14 | -38 | -5 |
| Cr | | | -1 | -7 | -2 | -37 | 2 |
| Fe | | | | -2 | -7 | -35 | 0 |
| Ni | | | | | -18 | -40 | -8 |
| V | | | | | | -48 | -1 |
| Si | | | | | | | -45 |

Table 3 Values of ΔH_{mix} , ΔS_{mix} , δ , VEC и Ω for HEAs of Al-Co-Cr-Fe-Mn-Ni-Si-V alloy system

| Alloy | ΔH_{mix} , kJ/mol | ΔS_{mix} , J/(mol·K) | δ | VEC | Ω |
|---|---------------------------|------------------------------|----------|------|----------|
| AlCoCrFe _{0.87} Mn _{0.03} NiSi _{0.1} V | -17.04 | 15.52 | 5.18 | 6.76 | 1.6 |
| AlCoCrFe _{1.87} Mn _{0.03} NiSi _{0.1} V | -14.6 | 15.18 | 4.96 | 6.94 | 1.84 |
| Al ₂ CoCrFe _{0.87} Mn _{0.03} NiSi _{0.1} V | -18.98 | 15.07 | 5.78 | 6.22 | 1.3 |
| Al ₂ CoCrFe _{1.87} Mn _{0.03} NiSi _{0.1} V | -16.81 | 14.97 | 5.66 | 6.45 | 1.48 |

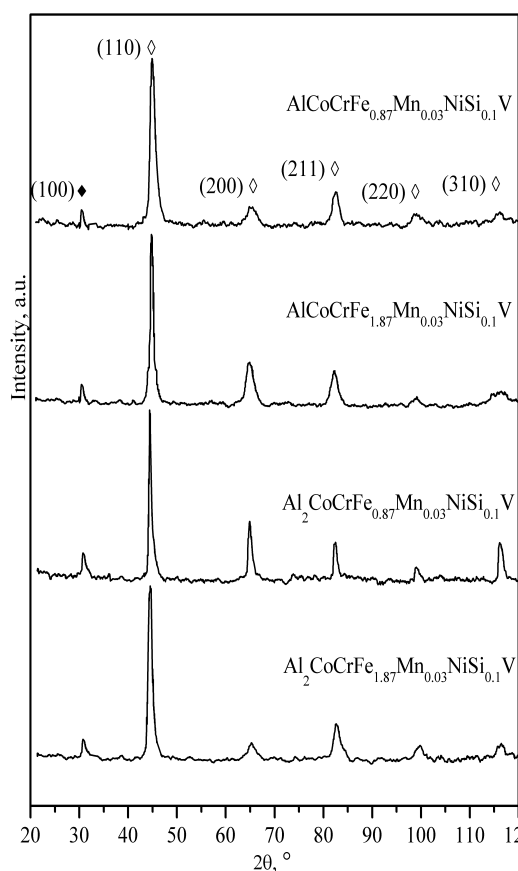


Fig.1. XRD patterns of as-cast HEAs of Al-Co-Cr-Fe-Mn-Ni-Si-V alloy system: ◇-BCC, ♦-B2.

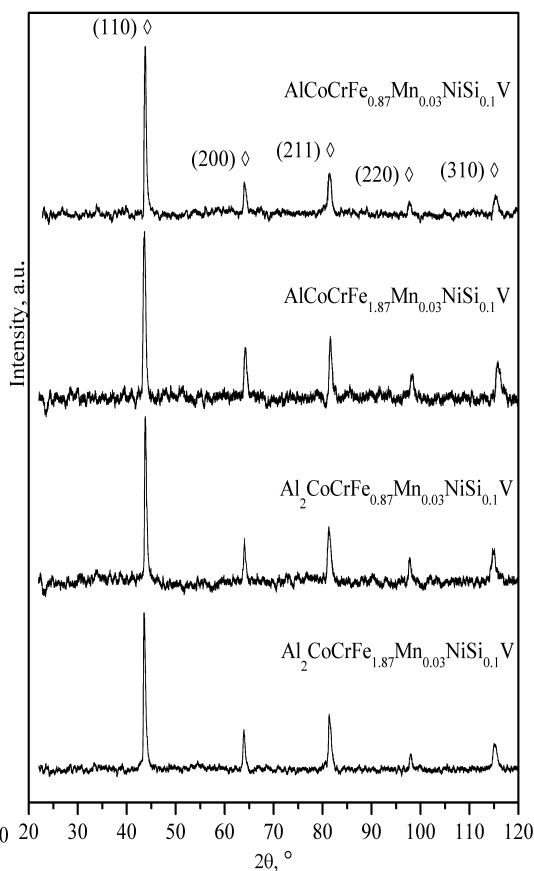


Fig.2. XRD patterns of splat-quenched HEAs of Al-Co-Cr-Fe-Mn-Ni-Si-V alloy system: ◇-BCC.

High microhardness values of Al-Co-Cr-Fe-Mn-Ni-Si-V HEAs can be explained by the presence of the dissimilar atoms of elements with different size, electronic structure and thermodynamic properties in the crystal lattice. This leads to significant distortion ($\Delta a/a$) of the crystal lattice. Consequently the hardness of the alloys increases. As seen

from Tab. 4, microhardness of the SQ alloys is higher than that of the as-cast alloys. This result is not unexpected, since the microstructure and the phase composition of the as-cast alloy after decomposition is in a more equilibrium multiphase state, while SQ alloys yields higher level of microstrains and dislocation density.

Table 4

Phase composition, coherent scattering areas (L), the degree of distortion of the crystal lattice ($\Delta a/a$), microhardness (H_u) and the dislocation density (ρ) of the investigated alloys

| Alloy | Phase composition | L , nm | $\Delta a/a$ | H_u , MPa | ρ , cm ⁻² |
|---|------------------------|----------|---------------------|-------------|---------------------------|
| As-cast AlCoCrFe _{0.87} Mn _{0.03} NiSi _{0.1} V | BCC + B2 (a=0.2888 nm) | 20±2 | $3.2 \cdot 10^{-3}$ | 6800±300 | $1.6 \cdot 10^{12}$ |
| SQ film AlCoCrFe _{0.87} Mn _{0.03} NiSi _{0.1} V | BCC (a=0.2882 nm) | 34±2 | $3.8 \cdot 10^{-3}$ | 6900±300 | $2.6 \cdot 10^{12}$ |
| As-cast AlCoCrFe _{1.87} Mn _{0.03} NiSi _{0.1} V | BCC + B2 (a=0.2882 nm) | 30±2 | $2.5 \cdot 10^{-3}$ | 4800±200 | $6.3 \cdot 10^{11}$ |
| SQ film AlCoCrFe _{1.87} Mn _{0.03} NiSi _{0.1} V | BCC (a=0.2879 nm) | 25±2 | $2.8 \cdot 10^{-3}$ | 6200±300 | $6.8 \cdot 10^{11}$ |
| As-cast Al ₂ CoCrFe _{0.87} Mn _{0.03} NiSi _{0.1} V | BCC + B2 (a=0.2888 nm) | 35±2 | $1.6 \cdot 10^{-3}$ | 6500±300 | $4.6 \cdot 10^{11}$ |
| SQ film Al ₂ CoCrFe _{0.87} Mn _{0.03} NiSi _{0.1} V | BCC (a=0.2887 nm) | 33±2 | $1.8 \cdot 10^{-3}$ | 7500±300 | $5.4 \cdot 10^{11}$ |
| As-cast Al ₂ CoCrFe _{1.87} Mn _{0.03} NiSi _{0.1} V | BCC + B2 (a=0.2886 nm) | 37±2 | $1.5 \cdot 10^{-3}$ | 4600±200 | $4.6 \cdot 10^{12}$ |
| SQ film Al ₂ CoCrFe _{1.87} Mn _{0.03} NiSi _{0.1} V | BCC (a=0.2881 nm) | 33±2 | $1.7 \cdot 10^{-3}$ | 5600±200 | $5.7 \cdot 10^{12}$ |

Fig. 3 is a SEM micrograph of the as-cast HEAs of Al-Co-Cr-Fe-Mn-Ni-Si-V system. All of the alloys display a typical cast dendritic structure with various configurations and volumes of the interdendritic space. The EDS analysis made it possible to reveal the dendritic segregation in alloys. The dendritic segregation area and interdendritic segregation area are denoted as DR and ID respectively (Fig.3). Table 5 shows the chemical composition of different areas analyzed by EDS. According to that, the bright DR area has a higher amount of Al and Ni than dark ID area, but the dark section of interconnected microstructure enriched with Fe, V and Cr elements. In contrast to the previous research [12], the addition of V element does not reduce segregation of Al, Ni, Fe, and Cr elements. Obviously, it is managed by Mn and Si.

Table 5

Chemical composition of as-cast HEAs of Al-Co-Cr-Fe-Mn-Ni-Si-V alloy system

| Alloy | | Elements, at. % | | | | | | | |
|---|---------------|-----------------|-------|-------|-------|------|-------|------|-------|
| | | Al | Co | Cr | Fe | Mn | Ni | Si | V |
| AlCoCrFe _{0.87} Mn _{0.03} NiSi _{0.1} V | Dendrite | 20.13 | 17.25 | 14.77 | 14.03 | 0.29 | 19.64 | 1.07 | 12.82 |
| | Interdendrite | 10.30 | 16.14 | 20.95 | 17.34 | 0.71 | 14.05 | 2.47 | 18.04 |
| | Nominal | 16.67 | 16.67 | 16.67 | 14.49 | 0.5 | 16.67 | 1.66 | 16.67 |
| AlCoCrFe _{1.87} Mn _{0.03} NiSi _{0.1} V | Dendrite | 15.71 | 14.08 | 13.91 | 26.23 | 0.42 | 15.48 | 1.19 | 15.38 |
| | Interdendrite | 11.46 | 14.37 | 16.71 | 27.85 | 0.47 | 13.81 | 1.61 | 13.72 |
| | Nominal | 14.28 | 14.28 | 14.28 | 26.74 | 0.43 | 14.28 | 1.43 | 14.28 |
| Al ₂ CoCrFe _{0.87} Mn _{0.03} NiSi _{0.1} V | Dendrite | 30.35 | 16.25 | 11.10 | 11.31 | 0.28 | 18.21 | 1.10 | 11.40 |
| | Interdendrite | 9.28 | 10.10 | 21.90 | 18.85 | 0.70 | 8.10 | 1.57 | 29.50 |
| | Nominal | 28.58 | 14.28 | 14.28 | 12.44 | 0.43 | 14.28 | 1.43 | 14.28 |
| Al ₂ CoCrFe _{1.87} Mn _{0.03} NiSi _{0.1} V | Dendrite | 30.03 | 11.8 | 11.25 | 21.04 | 0.27 | 13.47 | 0.96 | 11.08 |
| | Interdendrite | 9.97 | 15.8 | 15.32 | 25.02 | 0.57 | 10.63 | 1.49 | 21.11 |
| | Nominal | 25 | 12.5 | 12.5 | 23.37 | 0.38 | 12.5 | 1.25 | 12.5 |

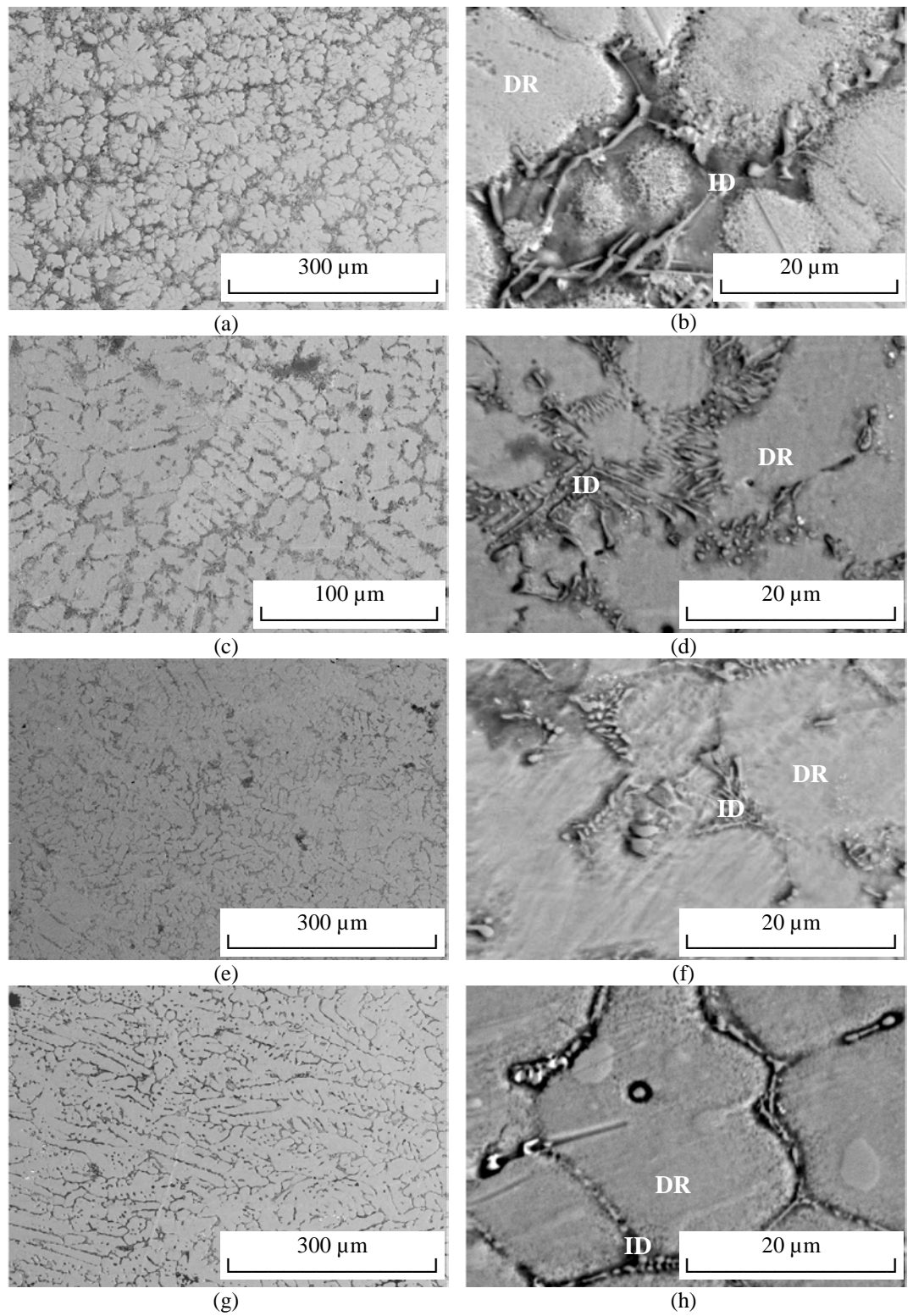


Fig.3. SEM images of as-casted HEAs specimens: (a), (b) - $\text{AlCoCrFe}_{0.87}\text{Mn}_{0.03}\text{NiSi}_{0.1}\text{V}$, (c),(d) - $\text{AlCoCrFe}_{1.87}\text{Mn}_{0.03}\text{NiSi}_{0.1}\text{V}$, (e), (f) - $\text{Al}_2\text{CoCrFe}_{0.87}\text{Mn}_{0.03}\text{NiSi}_{0.1}\text{V}$, (g),(h) - $\text{Al}_2\text{CoCrFe}_{1.87}\text{Mn}_{0.03}\text{NiSi}_{0.1}\text{V}$.

4. Conclusions

The following conclusions can be drawn on the base of the investigations of the Al-Co-Cr-Fe-Mn-Ni-Si-V HEA's produced in the as-cast and splat quenched state.

1. As-cast alloys have multiphase BCC + B2 structure, while SQ alloys exhibit only disordered BCC solid solution structure.
2. The level of microstrains, dislocation density and microhardness of Al-Co-Cr-Fe-Mn-Ni-Si-V HEA's increases with increasing a cooling rate.
3. The dominant role of the element with a higher melting temperature as the basis for the formation of solid solution in the studied alloys is confirmed.

References

1. **Murty, B.S.** High-entropy alloys [Text]/ B.S. Murty, J.W. Yeh, S. Ranganathan.– Oxford:Butterworth-Heinemann, 2014.–219p.
2. **Zhang, Y.** Solid-solution phase formation rules for multi-component alloys [Text]/ Y. Zhang, Y.J. Zhou, J.P.Lin, G.L. Chen, P.C. Liaw//Advanced Engineering Materials.–2008. –V.10, Iss. 6. –P. 534–538.
3. **Zhang, Y.** Alloy design and properties optimization of high-entropy alloys [Text]/ Y. Zhang, X.Yang, P.K. Liaw//JOM.–2012. –V.64, Iss. 7. –P. 830–838.
4. **Guo, S.** Phase stability in high entropy alloys: Formation of solid-solution phase or amorphous phase [Text]/S. Guo, C.T.Liu// Progress in Natural Science: Materials International.–2011.–V. 21, Iss. 6, –P. 433–446.
5. **Guo, S.** Effect of valence electron concentration on stability of fcc or bcc phase in high entropy alloys [Text]/S. Guo, C. Ng, J.Lu, C.T.Liu// Journal of Applied Physics.–2011.–V. 109, Iss. 10, –P. 103505-1–103505-5.
6. **Bashev, V. F.** Structure and properties of high entropy CoCrCuFeNiSn_x alloys [Text]/ V. F. Bashev, O. I. Kushnerov // The Physics of Metals and Metallography. –2014, –V. 115, No. 7,– P. 692–696.
7. **Zhang, Y.** Microstructures and properties of high-entropy alloys [Text]/ Y. Zhang, T.T. Zuo, Z. Tang, M.C. Gao, K.A. Dahmen, P.K. Liaw, Z.P. Lu // Progress in Materials Science. –2014. –V. 61.–P. 1-93.
8. **Tsai, M. H.** High-entropy alloys: A Critical Review/ M.H.Tsai, J.W. Yeh // Materials Research Letters.–2014,–V.2, Iss.3. –P.107-123.
9. **Stepanov, N. D.** Structure and mechanical properties of a light-weight AlNbTiV high entropy alloy [Text]/ N. D. Stepanov, D. G. Shaysultanov, G. A. Salishchev, M. A. Tikhonovsky // Materials Letters. – 2015.– Vol. 142.– P. 153–155.
10. **Takeuchi, A.** Classification of bulk metallic glasses by atomic size difference, heat of mixing and period of constituent elements and its application to characterization of the main alloying element [Text]/A. Takeuchi, A. Inoue// Materials Transactions.–2005. –V. 46 –P. 2817-2829.
11. **Singh A.K.** On the formation of disordered solid solutions in multi-component alloys [Text]/ A.K. Singh, A. Subramaniam// Journal of Alloys and Compounds. –2014. –V.587. –P. 113-119.
12. **Dong, Y.** Effect of vanadium addition on the microstructure and properties of AlCoCrFeNi high entropy alloy [Text]/ Y. Dong, K. Zhou, Y. Lu, X. Gao, T. Wang, T. Li // Materials & Design. – 2014. – Vol. 57. – P. 67–72.

Received 15.05.2015.